Preprint from

Proceedings of the 8th International Colloquium on Atomic Spectra and Oscillator Strengths

Madison, WI, 2005

An Electron Beam Ion Trap (EBIT) plus a microcalorimeter: a good combination for laboratory astrophysics

Joseph N. Tan[1], Eric Silver[2], Joshua Pomeroy[1], J. Martin Laming[3], and John Gillaspy[1]

[1]National Institute of Standards and Technology (NIST)
100 Bureau Drive, Gaithersburg, MD 20899

[2]Harvard-Smithsonian Center for Astrophysics
60 Garden Street, Cambridge, MA 02138

[3]Naval Research Laboratory, Code 7674L
Washington, DC 20375

Abstract

An EBIT can selectively create, in principle, any charge state of every naturally occurring element, has good control on atomic collision processes, and can produce nearly ideal conditions for the analysis of highly ionized plasmas of astrophysical importance. A microcalorimeter enables the broadband detection of X-ray emission with high energy resolution and near-unity quantum efficiency in the energy range wherein many cosmic X-ray sources emit the bulk of their energy (0.2 keV -10 keV). The combination (EBIT + microcalorimeter) provides a powerful tool for laboratory studies of the atomic/plasma processes underlying the energy release mechanisms in cosmic X-ray sources. We briefly describe some early experiments with a microcalorimeter built by the Smithsonian Astrophysical Observatory (SAO) and deployed on the NIST EBIT. We also present some very recent observations with a more advanced microcalorimeter built by SAO that can obtain an energy resolution of 4.5 eV. The higher spectral quality produced by the new system will be useful in laboratory measurements of interest in X-ray astronomy.

Key words: Electron beam ion trap, Microcalorimeter, X-ray, Highly charged ion

PACS: 52.70.-m; 34.80.Dp; 32.30.Rj; 34.50.Fa

1. Introduction

The "golden age of X-ray astronomy," as some have called it, is epitomized by the launches of the great orbiting observatories, *Chandra* in 1999 and *XMM-Newton* in 2000, revealing the hot Universe to human eyes in high spatial and spectral resolution. Startling discoveries about the details of the energetic processes in the universe have made frequent appearance in the mass media and captured the imagination of the public. In 2002, Riccardo Giacconi received the Nobel Prize in Physics for his contributions to the advancement of X-ray astronomy[1].

The discoveries that marked the birth of X-ray astronomy were made with relatively crude detectors (proportional and scintillation counters) deployed in sounding rockets and small satellites such as UHURU, SAS-3 and OSO-8. These early explorations found the first cosmic X-ray source (Scorpius X-1) [2], supernova remnants such as the Crab Nebula, neutron stars such as Hercules X-1 and the Crab pulsar, and countless other X-ray sources. These satellites were followed by the Einstein Observatory which carried the first imaging X-ray telescope for extra-solar observations [3].

These missions pushed the development of advanced X-ray instruments/techniques and established the importance of X-ray sources in astronomy and cosmology. X-ray photons from cosmic sources—with a few keV of energy or more—can penetrate vast distances comparable to the size of the Universe, and are well suited for probing the most distant objects from its earliest epochs. In fact, X-ray sources have been found in large numbers, in all categories of cosmic objects. Today, the modern orbiting X-ray observatories carry instruments that have many orders of magnitude higher capabilities. *Chandra*, for example, employs an X-ray focusing system with 0.5 arcsec resolution, high resolution imager/CCDs and nanofabricated transmission grating spectrometers to study cosmic X-ray sources with unprecedented sensitivity and precision. Currently, one of NASA's highest priorities for future missions is to launch even more powerful X-ray observatories—*Constellation-X,* for example—equipped with emerging technologies such as X-ray microcalorimeters, which are discussed in the section 2. The European Space Agency is considering similar efforts, like the planned *XEUS* mission.

Most of the 'visible' matter in the Universe is in a highly ionized state [4]; in particular, more than half of the baryonic mass in clusters of galaxies is to be found in hot plasmas tenuously pervading intergalactic space [1]. On Earth, however, highly ionized plasmas do not occur naturally. Before the 1980's the scientific study and application of highly ionized matter were limited by the extreme scarcity of laboratory access to highly charged ions. Today, powerful devices are available that can selectively make any ionization stage of any naturally occurring atom. Some of these devices are small enough to fit on a tabletop, such as the EBIT [5]. In section 3, we describe some unique features of the EBIT which are ideal for studying highly ionized plasmas of astrophysical interest. Some sources of highly charged ions are huge machines that produce ions with relativistic energies [6,7]. These two extremes—each having their own specialized applications—are complementary in providing a window into a large part of the universe that is still relatively unexplored and that can be expected to impact a variety of fields.

Shortly after *Chandra* and *XMM-Newton* began returning their first data, a long-anticipated problem could no longer be avoided: the well-controlled laboratory experiments that were needed to properly interpret the observatory data were not in place[8]. A burgeoning cornucopia of high-resolution X-ray observations is beset by some poorly understood high-energy processes responsible for the X-ray emissions, upon which depends the characterization of many cosmic sources[9]. The conditions in hot cosmic plasmas—such as elemental composition, ionization state, temperature distribution, and density—can be determined from X-ray spectroscopic measurements. A good understanding of physical processes in the hot universe—such as accretion, transport, shock waves, and atmospheric heating—requires knowledge of these basic parameters of the plasma. Complex models of the continuum and line emissions are involved in the determination of the plasma parameters; except in rare instances, the required atomic data are derived from theoretical calculations without experimental confirmation. Some uncertainties far exceed the precision of the X-ray observatory instruments. Fortunately, a few places have invested early in highly charged ion programs and these places are well-positioned to move quickly to provide the needed laboratory measurements—on the basis of which the theoretical calculations can be verified or refined to provide the best scientific interpretation of precious X-ray observatory data. In section 4, we discuss some EBIT plus microcalorimeter experiments of astrophysical interest.

2. Microcalorimeters: non-dispersive X-ray spectrometers

A radically new type of spectrometer based on microcalorimetry is being developed for future X-ray missions. Microcalorimeters do not disperse light to measure the wavelengths of its components. Rather, a microcalorimeter measures the energy of each photon by the amount of heat generated in an absorber at low temperature. The first microcalorimeter in space was flown on a sounding rocket [10]. It is expected that the Japanese will launch the ASTRO-E2 mission in 2005 [11], which will put into orbit a 6x6 microcalorimeter array with an energy resolution of 6 eV.

Microcalorimeters have important advantages over conventional X-ray detection systems. A microcalorimeter can measure the energy of an X-ray photon over a wide range of energy and angle of incidence, with near-unity quantum efficiency in the 2 keV to 10 keV energy band. Crystal and grating spectrometers can provide very high resolution, but they operate within more limited ranges of energy and angles of incidence, have much lower efficiency, and are difficult to use for imaging a source. Solid-state ionization detectors also can operate with high efficiency over a wide energy bandwidth and angle of incidence, but the energy resolving power is intrinsically limited to E/_E ~ 50. On the other hand, microcalorimeters have attained 2 eV to 3 eV resolution [12, 13]. To illustrate, we compare a spectrum from SiLi detector with that from a microcalorimeter in Fig.1—an emission line spectrum of argon ions confined in the NIST EBIT is observed (a) using a commercial SiLi detector, and (b) using a new microcalorimeter built by the Smithsonian Astrophysical Observatory.

As part of our joint laboratory astrophysics program, the NIST EBIT group collaborates with the Smithsonian Astrophysical Observatory (SAO) to develop microcalorimeters for experiments with highly charged ions in an electron beam ion trap (EBIT). A microcalorimeter is an ideal spectrometer for EBIT-type laboratory plasmas because, in addition to the desirable features indicated above, it is insensitive to the polarization of the X-ray emission associated with the well-defined quantization axis along the intense electron beam which excites the trapped ions. An advanced microcalorimeter deployed at NIST uses a two-stage Adiabatic Demagnetization Refrigerator (ADR) for cooling the detectors; it maintains an operating temperature of 60 mK for over 80,000 seconds before the ADR must be recycled. In the calorimeter, X-ray photons are absorbed in 0.35 mm x 0.35 mm x 7 μm size foils of superconducting tin and converted into heat. For a nominal heat capacity of 10^{-13} J/K, an absorbed 6 keV photon raises the temperature by 10 mK. The temperature rise is measured with a neutron transmutation-doped (NTD) germanium thermistor which is attached to the underside of the absorber. During data acquisition, the detectors are stabilized at 60 mK to within 5 μK. The NTD thermistor is impedance matched to a JFET negative voltage feedback circuit[14]. Designed for broad-band applications, the detector provides 95% quantum efficiency at 6 keV. An NTD-Ge microcalorimeter with a linear 1x4 array of Sn absorbers is being commissioned at the NIST EBIT facility. An energy resolution of 4.5 eV is obtained at the EBIT for this instrument (Fig. 2), while a resolution of 3.1 eV at 6 keV has been achieved under more optimal bench-top conditions at SAO[12].

3. The electron beam ion trap (EBIT)

An electron beam ion trap (EBIT) provides unique capabilities for studying the behavior of highly charged ions in hot plasmas, and for investigating how the atomic structure and plasma conditions influence the X-ray emission observed in cosmic sources. The EBIT can produce plasmas under nearly ideal conditions suited for analyzing astrophysical plasma conditions—*e.g.*, virtual absence of Doppler shift or broadening, a mono-energetic electron beam, etc.—and has good control over a wide range of experimental conditions to enable the creation of a comprehensive database of precise measurements for comparison with theoretical atomic physics calculations. As a unique tool in the X-ray regime and as a source of highly charged ions, the EBIT continues to find new applications. Soon after its inception through a collaboration between the Lawrence Livermore National Laboratory (LLNL) and the Lawrence Berkeley National Laboratory in 1985, NIST began operation of its EBIT in 1993. Today, there is a worldwide community of at least eight EBIT facilities, and several more being planned or under construction.

Detailed descriptions of the electron beam ion trap have been presented elsewhere[15]. In brief, the EBIT has been described as “the marriage of a cryogenic Penning trap with an … electron beam”[16]. The Penning trap[17] consists of the electric field produced by

potentials applied to three cylindrical electrodes (also called drift tubes), and a > 3 Tesla magnetic field produced by a pair of coaxial Helmholtz coils symmetrically positioned in the mid-plane of the central electrode. Liquid helium is used to make the Helmholtz coils superconducting and also to cool the trap surfaces for attaining an ultra-high vacuum environment. The electron beam is provided by a high perveance electron gun, focused through holes in the end-cap drift tubes along the symmetry axis, and compressed by the strong magnetic field to a beam radius of about 35 μm near the central region of the trap. The electron beam current (>100 mA) can be compressed to a current density of ~ 4000 A/cm^2, almost in the range of some vacuum arcs[18]—*but it is a continuous current in an EBIT*. In the presence of such an intense electron beam the dynamics of trapped ions does not resemble that in a Penning trap[19, 17], but contains features that are ideal for producing, trapping, and probing highly charged ions.

For instance, in most of the data presented here, the electron beam is accelerated to a kinetic energy of 5.1 keV at the center of the trap. An electron beam current in the range 80 mA to 90 mA is compressed by a co-axial magnetic field of 2.7 Tesla. Axial confinement is provided by a potential well depth of 280 V formed from two end-cap electrodes and a central electrode. The central electrode has eight slits, seven of which have clear line-of-sight access to viewports. Gaseous atomic species can be injected through one of the seven ports. Various spectrometers can be installed on the remaining viewports, aligned with the slits to collect photons emitted by the trapped ions—the new SAO microcalorimeter is positioned 74 cm from the center of the NIST EBIT. To maintain high purity of the species of interest, the ion trap is emptied every 1010 ms by momentarily raising the potential of the central electrode above those of the end-cap electrodes for 10 ms to invert the axial well. Some experiments will be discussed in the next section.

For X-ray spectroscopy and plasma studies, an EBIT has a number of attractive features. First, high ion densities—exceeding the Brillouin limit of a Penning trap in some cases—can be attained due to the stabilizing effects of the electron beam space charge. Second, charge state production is very selective because the electron beam is nearly mono-energetic. Atoms injected into the electron beam are ionized in a step-wise fashion—like peeling an onion—until the beam energy is not enough to lift the next deeper bound electron to the continuum. Third, the electronic states (*e.g.*, the energy levels) of trapped ions can be probed using the electron beam itself, which has an energy distribution as narrow as ~ 50 eV. Various atomic processes, such as excitation and dielectronic recombination, can be controlled precisely by fine tuning the electron beam acceleration. These capabilities of an EBIT, when added with those of a microcalorimeter, make an excellent tool for laboratory astrophysics.

4. Some experiments with a microcalorimeter on an EBIT

The NIST-SAO joint laboratory astrophysics program started in 1999, at about the time of the launch of the *Chandra* X-ray observatory. Here, some experiments with the first microcalorimeter deployed on the NIST EBIT are described briefly. A new SAO

microcalorimeter is presently being commissioned on the NIST EBIT. We present a few observations with the new system to illustrate the improvements; these are the first published observations with the new NTD-Ge microcalorimeter, although some preliminary results at the start of commissioning were announced earlier[20].

One of the first X-ray microcalorimeter experiments was to use the brightest X-ray diagnostic lines in He-like ions to verify that the electron densities inferred from the line intensity ratios for different species trapped simultaneously in an EBIT agree with each other and are consistent with the nominal densities of the electron beam estimated from the known conditions[8]. The diagnostic scheme, due to Gabriel and Jordan[21], is based upon the relativistic magnetic dipole (M1) transition of the 1s2s $^3S_1$ excited state to the ground state ($1s^2\ ^1S_0$) with the emission of one photon. Figure 3 shows a simplified level diagram for the n = 2 → 1 transitions in the helium isoelectronic series. The 1s2s $^1S_0$ excited state decays to the ground state via a parity-changing, two-photon transition. The electric-dipole allowed (E1) decay of the 1s2p $^1P_1$ excited state gives an emission line which is called the 'resonance line' and conventionally labeled '**W**'. The intercombination lines (**X**+**Y**) come from transitions of the 1s2p $^3P_2$ and 1s2p $^3P_1$ states to the ground state. And lastly, the one-photon decay from the 1s2s $^3S_1$ state via relativistic M1 transition gives the 'forbidden line **Z**'. Although labeled as 'forbidden,' the relativistic M1 transition is the dominant decay mode of the 1s2s $^3S_1$ state, with a rate which can be many orders of magnitude larger than the two-photon decay rate. For nearly 30 years, however, the one-photon decay was underestimated to be generally much weaker than the two-photon decay, until evidence of its dominant strength appeared around 1969 in the soft X-ray spectra of the solar corona[21].

The line intensity ratios formed from the resonance, intercombination and forbidden lines in He-like ions are used widely as density and temperature diagnostics in both photoionized and collisionally-ionized astrophysical plasmas. In particular, the diagnostic line ratios from the He-like N VI, O VII, Ne IX and Mg XI ions are especially important for determining the electron density in hot plasmas. Using the same symbols **W**, **X**, **Y**, and **Z** to denote the corresponding intensities of these emission lines, we write the density-sensitive ratio $\mathbf{R} = \mathbf{Z}/(\mathbf{X}+\mathbf{Y})$, and the temperature-sensitive ratio $\mathbf{G} = (\mathbf{X}+\mathbf{Y}+\mathbf{Z})/\mathbf{W}$. As a function of electron density, the line intensity ratio **R** is constant in the low-density regime. When the electron density is high enough, the rate of electron impact excitation from the 1s2s $^3S_1$ state into the 1s2p ^3P states can compete effectively with the rate of the relativistic M1 decay; hence, the ratio **R** is reduced, decreasing with further increase in the electron density as the population in the 1s2s $^3S_1$ state is depleted via the electron-ion collisional transfers. The sensitivity of R as a density diagnostic depends on the one-photon decay lifetime τ of the 1s2s $^3S_1$ state, which spans the range from 9×10^3 s in He to 2×10^{-10} s in Kr^{34+} ions—τ scaling roughly as Z^{-10} within a wide range of atomic number Z [22]. The He-like lines of N VI, O VII, and Ne IX are most sensitive in the density range 10^{10} cm^{-3}—10^{12} cm^{-3}, and hence, were used in the experiments with the NIST EBIT (wherein electron beam densities can go as high as 5×10^{12} cm^{-3}). Although there are some subtleties[23, 24], the atomic structure of He-like ions is relatively simple, and the theoretical calculations for their X-ray diagnostic lines are among the most accurate in general (but not all have been benchmarked).

Another experiment involved the emission lines of the neon-like Fe XVII (or Fe^{16+}). Since iron is the endpoint of nucleosynthesis in stellar cores, it is an abundant element in cosmic X-ray sources. Emission lines of Fe XVII are among the strongest observed in the line spectra of astrophysical plasmas with temperatures around 5 x 10^6 K. Of the six most prominent lines, three originate from transitions to the $^1S_0$ ground state (closed $2p^6$ shell) from the $2p^5 3s$ configuration—i.e., decays of the $^1P_1$, $^3P_1$, and $^3P_2$ excited states. The other three lines come from transitions to the $^1S_0$ ground state from the $2p^5 3d$ configuration—i.e., decays of the $^1P_1$, $^3D_1$, and $^3P_1$ excited states. Although more complex than He-like transitions, these lines could potentially provide excellent electron temperature diagnostics[25]. However, discrepancies involving the intensity ratios were found in the observations of solar flares[26] and astrophysical sources[27, 28]. Recently, laboratory measurements were made by the EBIT groups at LLNL[29, 30] and NIST[31], and improved theoretical calculations have been completed[32, 33, 34]. We are preparing to investigate some of the new predictions and remaining discrepancies[30,35,34], using the new NTD-Ge microcalorimeter.

In addition, using the first SAO microcalorimeter, a broadband survey of key X-ray diagnostic lines in N, O, Ne, Ar and Kr has been obtained from various charge states of these ions[8]. This included the *K* emissions from nitrogen, oxygen, and neon; *K* and *L* emissions from argon; and *L* emission from krypton. By way of introducing the new NTD-Ge microcalorimeter, Fig. 1(b) and Figs. 4-6 show a similar survey using the most recent observations with the new microcalorimeter that obtained an energy resolution of 4.5 eV. They give an indication of the higher spectral quality. In the Kr spectrum (Fig. 6), for example, more distinct lines and finer spectral features are clearly observed by comparison with the earlier survey using the first SAO microcalorimeter with ~ 6 eV resolution[8]. Other improvements such as recent advances in metal vapor vacuum arc (MeVVA) ion source technology[36] will also be useful in laboratory astrophysics experiments underway.

5. Summary

Chandra and *XMM-Newton* have ushered in a new era in X-ray astronomy. The lack of well-controlled laboratory measurements for proper interpretation of observatory data becomes acute in the wake of many advances that their unprecedented capabilities are enabling in various areas of astronomy. An electron beam ion trap (EBIT) can create any charge state of every naturally occurring element[38], and provide nearly ideal, controlled conditions for the analysis of highly ionized plasmas of astrophysical importance. Microcalorimetry, a new type of X-ray spectrometry which does not disperse light, is emerging as a valuable technique because of its all-around good performance in the broadband detection of X-ray photons with high energy resolution and near-unity quantum efficiency. An EBIT and a microcalorimeter form a good combination that makes laboratory experiments feasible to study the atomic/plasma physics relevant to understanding the energy release mechanisms at work in cosmic X-ray sources.

6. References

[1] Giacconi, R., "The Dawn of X-ray Astronomy," Nobel Lecture, December 9, 2002.

[2] Giacconi, R., Gursky, H., Paolini, F. & Rossi, B., Phys. Rev. Lett. **9**, 439(1962).

[3] Bradt, H.V.D., Ohashi, T., Pounds, K.A., Annu. Rev. Astron. Astrophys. **30,** 391(1992).

[4] Fang, T.T., and Canizares, C.R., Astrophys. J. **539,** 532(2000).

[5] Levine, M.A., Marrs, R.E., Henderson, J.R., Knapp, D.A., and Schneider, M.B., Phys. Scr. T **22,** 157(1988).

[6] Stohlker, T., *et al*., Phys. Rev. Lett. **85,** 3109(2000).

[7] Angert, N., Nucl. Tracks Rad. Meas. **19,** 871(1991).

[8] Silver, E., Schnopper, H., Bandler, S., Brickhouse, N., Murray, S., Barbera, M., Takacs, E., Gillaspy, J.D., Porto, J.V., Kink, I., Laming, J.M., Madden, N., Landis, D., Beeman, J., and Haller, E.E., Astrophys. J. **541,** 495(200).

[9] Blandford, R.D., Phil. Trans. R. Soc. Lond. A **360,** 2091(2002).

[10] Porter, F.S.; Figueroa, E.; Kelley, R.L.; Stahle, C.K.; Szymkowiak, A.E.; Almy, R.; Apodaca, E.; Galeazzi, M.; McCammon, D.; Sanders, W.; Nucl. Instrum. Meth. in Phys. Res. A, **444**, 220(2000).

[11]Kelley, *et al*,Nucl. Instrum. Meth. in Phys. Res. **A**, **520**, 364(2004).

[12] Silver, E., Austin, G., Beeman, J., Goulding, F., Haller, E.E., Landis, D., and Madden, N., accepted for publication in Nucl. Instrum. and Meth. in Phys. Res. (2005).

[13] See review by Twerenbold, D., Rep. Prog. Phys. **59,** 349(1996).

[14] Silver, E., Labov, S., Goulding, F., Madden, N., Landis, D., Beeman, J., Pfafman, T., Melkonian, L., Millet, I., Vai, Y., SPIE **1159,** 423(1989).

[15] See, for example, Currell, F.J., "Trapping Highly Charged Ions: Fundamentals and Applications." (Edited by Gillaspy, J.,) (Nova Science Publishers, Inc., Huntington, New York, 2001). p3; and references therein.

[16] Marrs, R.E., "Remembering Mort Levine and the beginning of the EBIT," NIST Special Publication **972,** xvii(2001).

[17] See review by Brown, L.S., and Gabrielse, G., Rev. Mod. Phys. **58,** 233(1986).

[18] Harris, L.P., "Vacuum Arcs: Theory and Applications." (Edited by Lafferty, J.M.,)(John Wiley & Sons, New York, 1980). p120.

[19] Davidson, R.C., "An Introduction to the Physics of Nonneutral Plasmas." (Addison-Wesley Publishing Co.)(1990).

[20] Gillaspy, J.D., Blagojevic, B., Dalgarno, A., Fahey, K., Kharchenko, V., Laming, J.M., Le Bigot, E.-O., Lugosi, L., Makonyi, K., Ratliff, L.P., Schnopper, H.W., Silver, E.H., Takacs, E., Tan, J.N., Tawara, H., Tokesi, K., "Atomic Processes in Plasmas: 14th APS Topical Conference on Atomic Processes in Plasmas." (Edited by Cohen, J.S., Mazevet, S., Kilcrease, D.P.,)(AIP, New York, 2004). p 245.

[21] Gabriel, A., and Jordan, C., MNRAS **145,** 241(1969).

[22] Sucher, J., Rep. Prog. Phys. **41**, 1781(1978) provides a review of the theory of M1 transitions and their role in atomic and particle physics.

[23] Phillips, K.J.H., Greer, C.J., Bhatia, A.K., Coffey, I.H., Barnsley, R., Keenan, F.P., Astron. Astrophys. **324,** 381(1997).

[24] Brickhouse, N.S., Dupree, A.K., Edgar, R.J., Liedahl, D.A., Drake, S.A., White, N.E., Singh, K.P., Astrophs. J. **530,** 387(2000).

[25] Raymond, J.C., and Smith, B.W., Astrophys. J. **306,** 762(1986).

[26] Schmelz, J.T., Saba, J.L.R., Strong, K.T., Astrophys. J. Lett. **398,** L115(1992).

[27] Brinkman, A.C., Bunsing, C.J.T., Kaastra, J.S., Van Der Meer, R.L.J., Meve, R., Paerels, F., Raasen, A.J.J., Van Rooijen, J.J., Brauninger, H., Burkert, W., *et al.*, Astrophys. J. Lett. **530,** L111(2000).

[28] Canizares, C.R., Huenemoerder, D.P., Davis, D.S., Dewey, D., Flanagan, K.A., Houck, J., Markert, T.H., Marshall, H.L., Schattenburg, M.L., Schulz, N.S., *et al.*, Astrophys. J. Lett. **539,** L41(2000).

[29] Brown, G.V., Beiersdorfer, P., Boyce, K.R., Gendreau, K.C., Gu, M.F., Gygax, J., Kahn, S.M., Kelley, R., Porter, F.S., Savin, D.W., Utter, S.B., Phys. Scr. T **92**, 130 (2001).

[30] Beiersdorfer, P., Behar, E., Boyce, K.R., Brown, G.V., Chen, H., Gendrerau, K.C., Gu, M.F., Gygax, J., Kahn, S.M., Kelley, R.L., Porter, F.S., Stahle, C.K., and Szymkowiak, A.E., Astrophys. J. **576,** L169(2002).

[31] Laming, J.M., Kink, I., Takacs, E., Porto, J.V., Gillaspy, J.D., Silver, E.H., Schnopper, H.W., Bandler, S.R., Brickhouse, N.S., Murray, S.S., Barbera, M., Bhatia, A.K., Doschek, G.A., Madden, N., Landis, D., Beeman, J., and Haller, E.E., Astrophys. J. **545,** L161(2000).

[32] Doron, R., Behar, E., Astrophys. J. **574,** 518(2002).

[33] Chen, G.X., Pradhan, A.K., Phys. Rev. Lett. **89,** 013202(2002).

[34] Chen, G.X., Pradhan, A.K., private communication.

[35] Takacs, E., Silver, E., Laming, J.M., Gillaspy, J.D., Schnopper, H., Brickhouse, N., Barbera, M., Mantraga, M., Ratliff, L.P., Tawara, H., K. Makonyi, K., Madden, N., Landis, D., Beeman, J., Haller, E.E., Nucl. Instr. Meth. B **205,** 144(2003).

[36] Holland, G.E., Boyer, C.N., Seely, J.F., Tan, J.N., Pomeroy, J., Gillaspy, J.D., submitted to Rev. Sci. Instr.

[37] I. Kink, J.M. Laming, E. Takacs, J.V. Porto, J.D. Gillaspy, E. Silver, H. Schnopper, S.R. Bandler, M. Barbera, N. Brickhouse, S. Murray, N. Madden, D. Landis, J. Beeman and E.E. Haller, Phys. Scr. **T92,** 454(2001).

[38] Marrs, R.E., Elliott, S.R., and Knapp, D.A., Phys. Rev. Lett. **72**, 4082(1994).

Figures

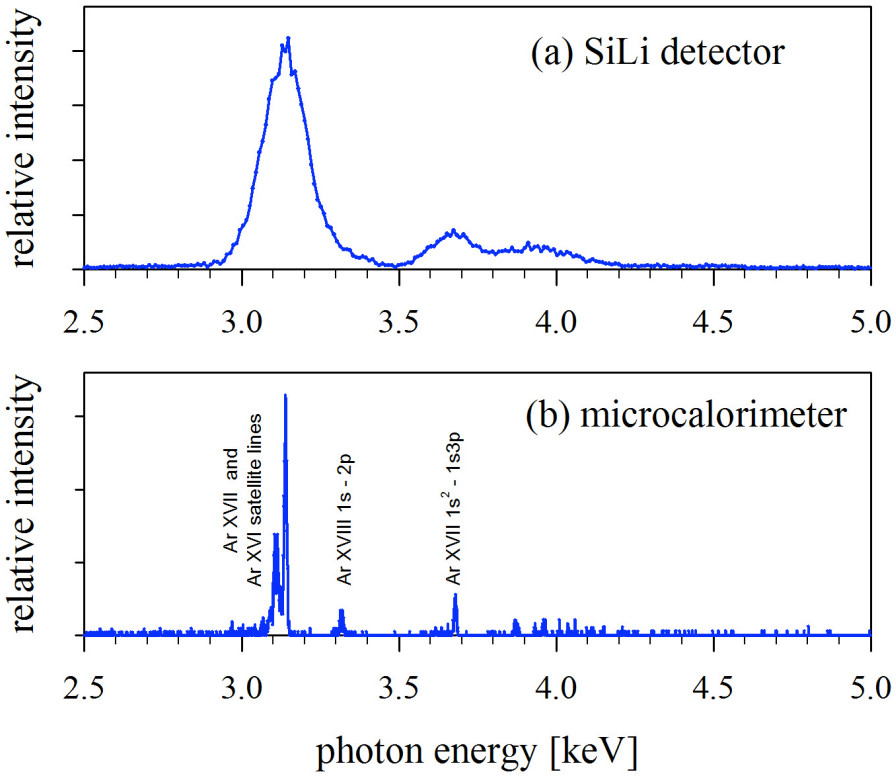

Figure 1

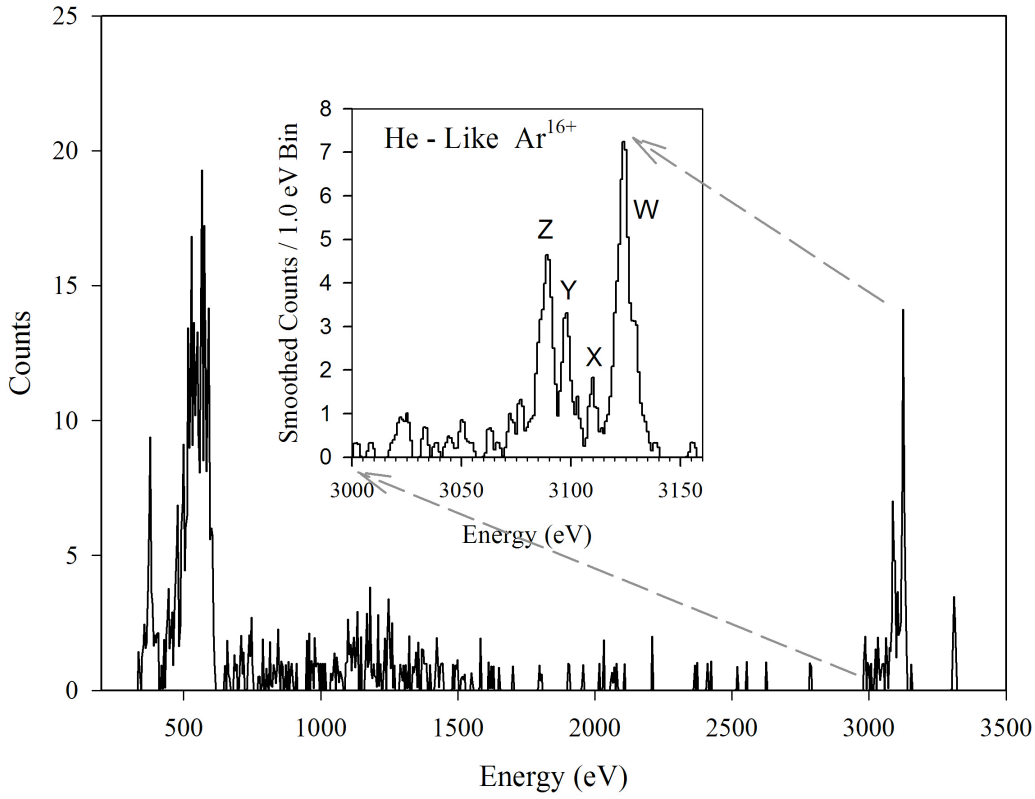
Counts
Energy (eV)
He - Like Ar16+
Smoothed Counts / 1.0 eV Bin
Energy (eV)
Z
Y
X
W

Figure 2

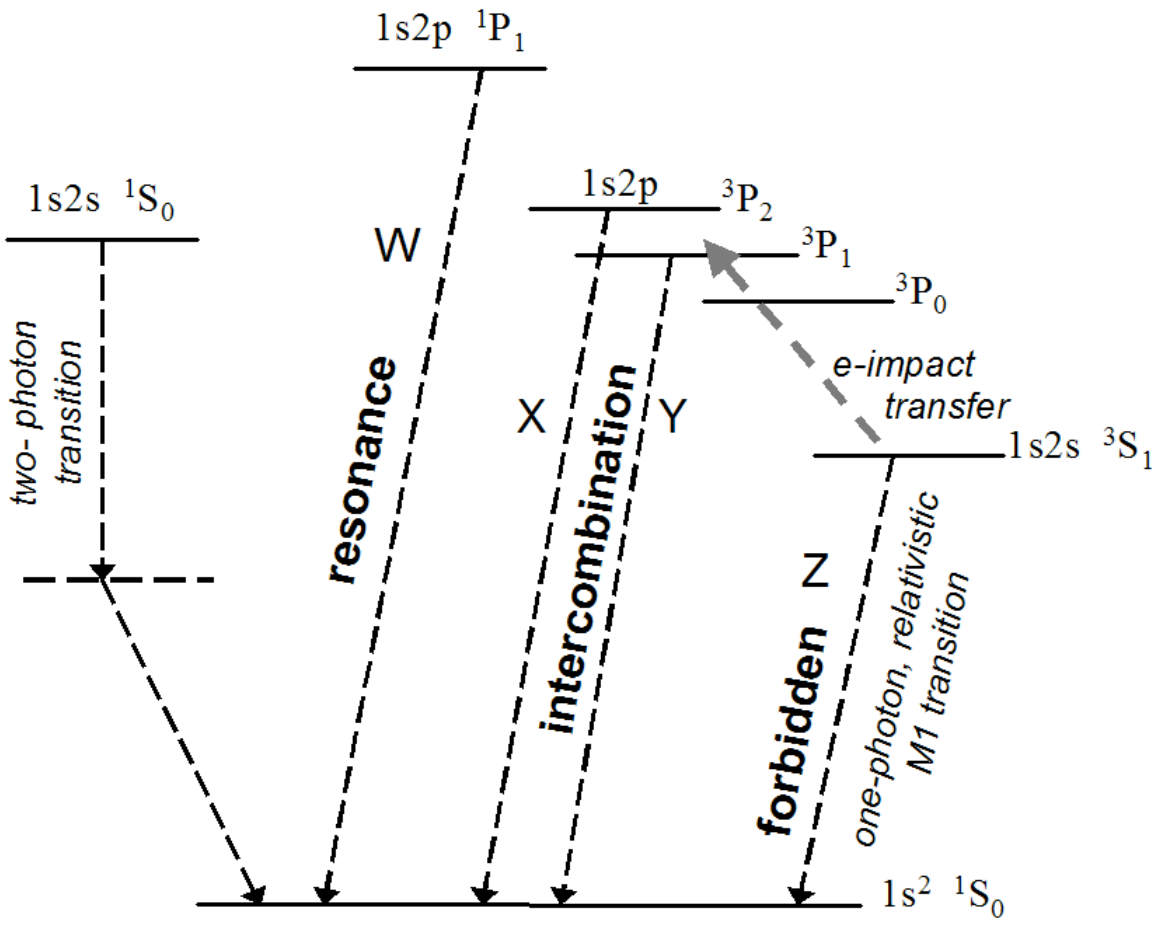
1s2p $^1P_1$
1s2s $^1S_0$
1s2p $^3P_2$
$^3P_1$
$^3P_0$
W
X
Y
Z
two- photon transition
resonance
intercombination
e-impact transfer
1s2s $^3S_1$
forbidden
one-photon, relativistic M1 transition
$1s^2$ $^1S_0$

Figure 3

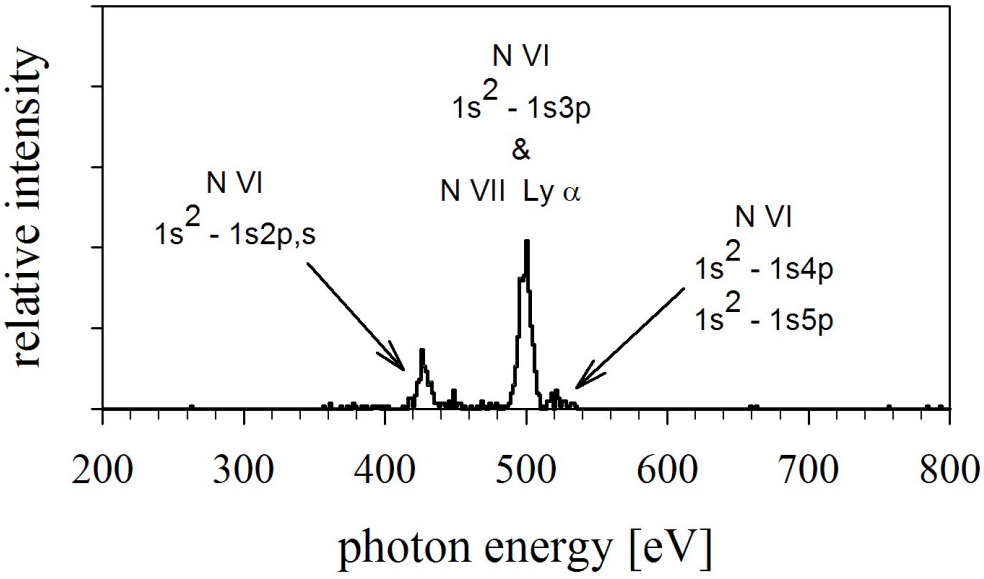
relative intensity
N VI
1s2 - 1s3p
&
N VII Ly α
N VI
1s2 - 1s2p,s
N VI
1s2 - 1s4p
1s2 - 1s5p
200
300
400
500
600
700
800
photon energy [eV]

Figure 4

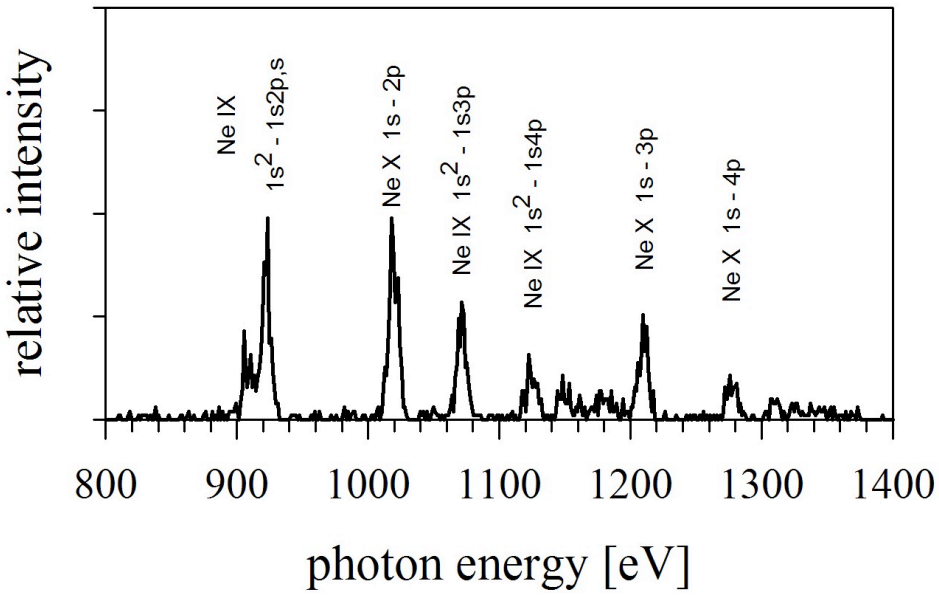
relative intensity
Ne IX
1s2 - 1s2p,s
Ne X 1s - 2p
Ne IX 1s2 - 1s3p
Ne IX 1s2 - 1s4p
Ne X 1s - 3p
Ne X 1s - 4p
800
900
1000
1100
1200
1300
1400
photon energy [eV]

Figure 5

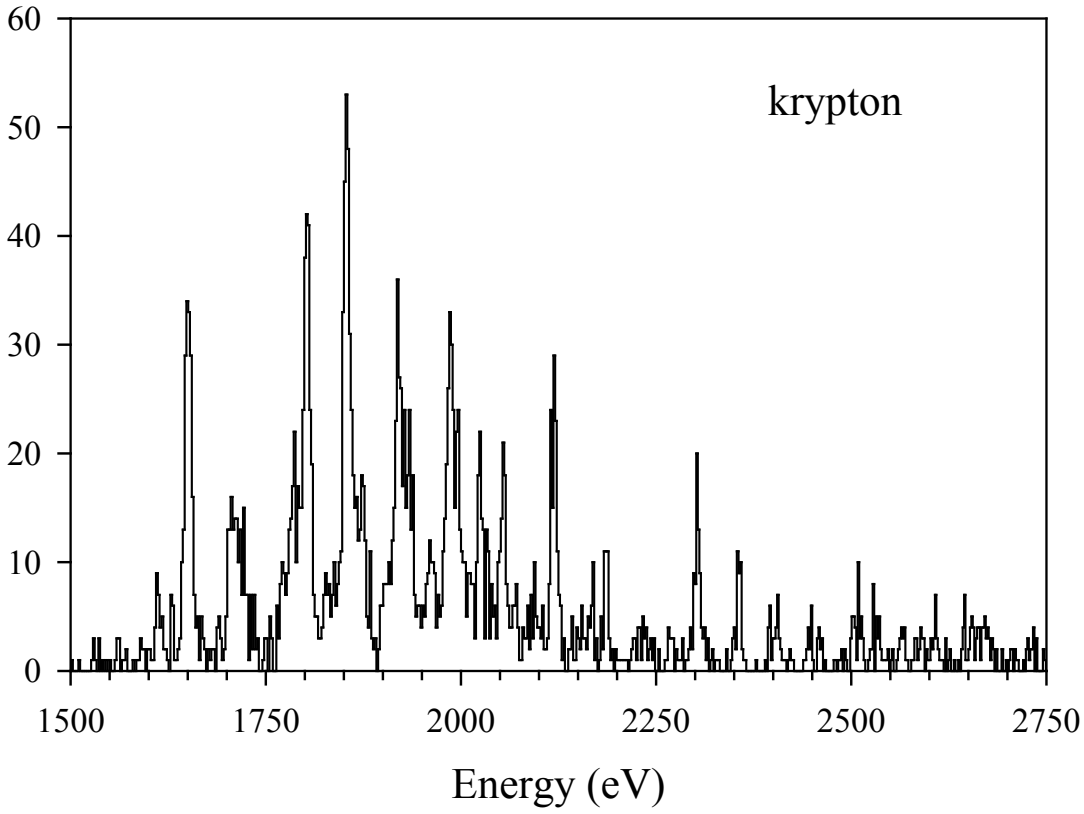
60
50
40
30
20
10
0
krypton
1500
1750
2000
2250
2500
2750
Energy (eV)

Figure 6

Figure caption

Figure 1. Comparison between a solid-state ionization detector and a microcalorimeter. X-ray spectra of argon ions confined and excited in the NIST EBIT are taken using (a) a commercial SiLi detector, and (b) a microcalorimeter developed by SAO.

Figure 2. Microcalorimeter spectrum from argon ions confined in the NIST EBIT. The emission line spectrum from helium-like Ar^{16+} is in the inset with the energy scale magnified to show the resonance, intercombination and forbidden lines resolved. This data set taken shortly after first light indicates that the energy resolution is > 4.5 eV.

Figure 3. A simplified level diagram for the n = 2 → 1 transitions in the helium isoelectronic series. The 1s2s $^1S_0$ excited state decays via a two-photon transition. The electric-dipole allowed (E1) decay of the 1s2p $^1P_1$ excited state gives the resonance line W. The intercombination line (X+Y) comes from transitions of the 1s2p $^3P_2$ and 1s2p $^3P_1$ states to the ground state. The forbidden line Z comes from the one-photon decay of the 1s2s $^3S_1$ excited state via relativistic M1 transition.

Figure 4. Microcalorimeter spectrum of emission lines from nitrogen injected into the NIST EBIT. The nitrogen ions are trapped in the EBIT, and excited by an 85 mA electron beam which is accelerated to 5.1 keV.

Figure 5. Microcalorimeter spectrum from neon ions excited in the EBIT, showing many lines from He-like and H-like (Ly-α) transitions.

Figure 6. A spectrum of krypton emission lines observed with a microcalorimeter on the NIST EBIT. The krypton ions are excited by an 82 mA electron beam with 5.1 keV energy. Identification of the Kr charge states for some of the emission lines can be found in Ref. [37].